A Hybrid Approach to Classify Power Quality Problems in Distribution Systems

DOI : 10.36909/jer.10717

Okan Ozgonenel*, Kubra Nur Akpinar

Electric and Electronic Engineering, Ondokuz Mayis University, Samsun, 55200, Turkey.

*Email: okanoz@omu.edu.tr; Corresponding Author.

ABSTRACT

Electrical power systems are expected to transmit continuously nominal rated sinusoidal voltage and current to consumers. However, the widespread use of power electronics has brought power quality problems. This study performs classification of power quality disturbances using an artificial neural network (ANN). The most appropriate ANN structure was determined using the Box-Behnken experimental design method. Nine types of disturbance (no fault, voltage sag, voltage, swell, flicker, harmonics, transient, DC component, electromagnetic interference, instant interruption) were investigated in computer simulations. The feature vectors used in the identification of the different types of disturbances were produced using the discrete wavelet transform and principal component analysis. Our results show that the optimized feed forward multilayer ANN structure successfully distinguishes power quality disturbances in simulation data and was also able to identify these disturbances in real time data from substations.

Key words: power quality (PQ); optimization; disturbance; artificial neural network (ANN); experimental design

1. INTRODUCTION

Power quality disturbance is a problem resulting from the fluctuations in frequency and voltage that have arisen from the increasing dependency on nonlinear loads. Several types of power quality (PQ) disturbance can occur at any point in an electrical network during the operation of the system; this includes voltage sag/swell, harmonics, transient state, flicker, load switching and effects due to the widespread use of non-linear electronic loads. Electricity companies are implementing system audit, monitoring and power quality studies in order to characterize each power quality problem. The classification of different power quality disturbances helps to explain the failures of different types of load connected to the power system. The signal waveform provides an effective way to classify disturbances, but extracting this information by type of disturbance requires intensive computational processing. In general, signal analysis, feature extraction, and classification techniques are used to identify power quality disturbances. Feature selection is a key element in this approach, as unimportant features can be identified and ignored.

Several techniques including wavelet transform, short-term Fourier transform, Gabor-Winger transform, and S-transform have been applied to identify and classify power quality disturbances. In these studies, extraction of the wavelet was based on the energy distribution within the distortion and used multiple resolution analysis that was specific for each type of disturbance. Mallat's discrete wavelet transform technique allows various features of a signal to be extracted using multiple resolution analysis to divide the features into different frequency regions. Several methods have been proposed for the classification of PQ disturbances. Time frequency analysis, decision trees, support vector mechanisms, genetic algorithm, fuzzy logic, local weighted projection regression, artificial neural networks (ANN) are the most frequently used methods. ANN generally gives the best results compared to other classification methods and is largely immune to the effects of noise, however there is some difficulty in the selection

of feature parameters (frequency component, waveform) and the creation of the ANN structure is a complex process (Saxena et al., 2012).

The purpose of PQ disturbance detection is to identify the type of disturbance and develop control strategies. Mathematical algorithms such as Wavelet transform, Stockwell transform, Hilbert-Huang transform can be used to extract Eigenvectors. Artificial intelligence tools such as artificial neural networks, support vector machines, decision trees, and fuzzy logic may then be used to classify the disturbances.

The discrete wavelet transform (DWT) is frequently used to extract the features for voltage sag/swell, transients, interruption, and other features of sine based waveforms. ANN and fuzzy logic methods have been applied separately for the classification of the disturbances (Choong et al., 2005). Devaraj et al. analyzed voltage sag/swell, transients, and harmonic and flicker disturbances using the discrete Fourier transform. For this purpose an ANN was trained using the difference in phase angle, minimum difference in frequency between basic and test frequency, and the energy level of the wavelet coefficients (Devaraj et al., 2008).

Pozzebon et al. applied the DWT to detect pure sine wave, the transient condition occurring at switching time, flicker, harmonic, interruption, notch, and voltage sag. To increase speed of execution, principal component analysis (PCA) and radial based function ANN were used for classification (Pozzebon et al., 2010). Rodríguez et al. performed multiple resolution DWT analysis to detect disturbances and achieved 92% classification success with back propagation and probabilistic ANN (Rodríguez et al., 2010). Chandrasekar et al. used simulated data in the MATLAB / Simulink environment and tested their methodologies using the IEEE 6 bus test system. They achieved 95% classification success by using regulated DWT and ANN with bidirectional associative memory (Chandrasekar et al., 2010). Uyar et al. developed a pattern recognition approach to classify the deterioration in power quality in ATP-EMTP. Db8 was used as the mother wavelet, SVM method for classification, and 97% performance was achieved (Uyar et al., 2008). Elango et al. classified the power quality disturbance data received from a

textile factory by applying the Hilbert Huang Transform and three different ANN structures. They stated that radial basis function (RBF) and locally weighted projection regression (LWPR) have higher performance and faster classification than back propagation algorithm (BPA) for power quality disturbance identification. (Elango et al., 2011). Ijaz et al. analyzed PQ disturbances with DWT and used the energies of the DWT shape and scale coefficients as feature vectors. These feature vectors are applied as input to the artificial neural network, with the weights being improved by the differential evolutionary algorithm (Ijaz et al., 2015). Shilpa et al. achieved high classification performance by using SVM by applying Hilbert Huang Transform and experimental mode separation and collective experimental mode separation to detect voltage sag/swell, transient condition, and harmonic disturbances (Shilpa et al., 2015) . Liu et al. extracted features with the Stockwell transform and classified the disturbance data using the Takagi-Sugeno (TS) fuzzy logic method (Liu et al., 2015). Dalai et al. used the XWT (cross wavelet transform) supported by the Fisher linear discriminant analysis based method for feature extraction from distorted signals. A linear support vector machine based classifier core was found to be sufficient for the classification of extracted properties (Dalai et al., 2015).

Karasu et al. determined PQ disturbances by using statistical properties of the wavelet transform and the norm entropy method. The most appropriate features were found using the sequential advanced selection algorithm. The performance of support vector machines, multi-layer sensor, k nearest neighbor, and random subspace k closest neighbor classification algorithms, which are methods of working together, were investigated. The highest performance achieved was 99.3% accuracy, using the k nearest neighbor classification method (Karasu et al., 2016).

Perez et al. applied a new method and obtained the alpha, beta and zero components by applying the Clarke transformation to the disturbance sine wave (single line to ground and phase to phase faults) and the wavelet transform to the space-vector magnitudes and zero sequence component to calculate the energy distribution at wavelet detail levels (Perez et al., 2016).

Mejia-Barron et al. developed a phasor measurement unit based on power quality disturbances. After measuring the phasor and applying the P filter, they set the defect classification by determining the limit values with ANN and rule-based software (Mejia-Barron et al., 2017).

Mohan et al. used deep learning methods without any feature extraction to classify PQ disturbances. Convolutional neural network, recurrent neural network, identity recurrent neural network, long short term memory, gated repeating units, and convolutional neural network long term short term memory (CNN- LSTM) deep learning methods were used and CNN-LSTM had highest performance for classification (Mohan et al., 2017).

Das et al. classified PQ disturbances with fuzzy decision trees (FDT) after feature extraction with HHT (Hilbert-Huang Transform) conversion, EMD (empirical mode decomposition) and IMF (Intrinsic Mode Function) (Das et al., 2017).

Singh et al. used the non-dominant classification genetic algorithm (NSGA-II), which provides different Pareto optimal solutions for the most appropriate feature selection in the classification of PQ disturbances. They used S transformation for feature extraction, utilized decision trees in classification, and achieved 99.93% success (Singh et al., 2017).

Camarillo-Penaaranda et al. obtained the αβ components by applying Clarke transformation to the disturbance signal and performed the disturbance detection and classification according to the visual change in the phase angles of the components in the ellipse representation of voltage sag/swell, harmonics, noise and DC component and phase disturbances (Camarillo-Penaaranda et al., 2018).

The literature clearly shows the importance of obtaining feature vectors for the classification of PQ disturbances. The different classification methods gave varying performance in identifying each type of disturbance. ANN was the most used classification type, giving the highest performance, although network design was time-consuming due to the trial and error method of training.

This study uses the Box-Behnken response surface as analysis method, one of the experimental design methods to facilitate the ANN design phase. The number of hidden layers and neurons that make up the artificial neural network, the activation functions used and the appropriate parameters in the back propagation algorithms were selected using ANOVA statistical analysis. In this way, the most appropriate problem-based ANN structure was obtained and used in the classification of PQ disturbances.

2. MATERIAL AND METHOD

A hybrid algorithm consisting of principal component analysis, DWT and FFT to extract features for the detection of PQ disturbances and ANN for classification was used. The sine wave was used to represent the normal state, and after applying wavelet analysis to disturbance data, the coefficients were compared with the normal sine wave, and the type of disturbance was determined. As the wavelet coefficients were in the range of 49.5 - 50.5 Hz, principal components analysis was also applied in order to prevent false detection of the case of voltage sag/swell. Local maximum and minimum values were calculated by taking the envelope of each signal at the decision stage.

Selection of the parameters of the ANN are important in order to achieve high performance of classfication, and determining the number of neurons according to the number of input and unknown input layers can be time-consuming, and must be adjusted according to the desired output. Box-Behnken design was exploited in the ANN design phase.

The steps taken to identify and classify PQ disturbances in distribution systems are shown in Figure 1.

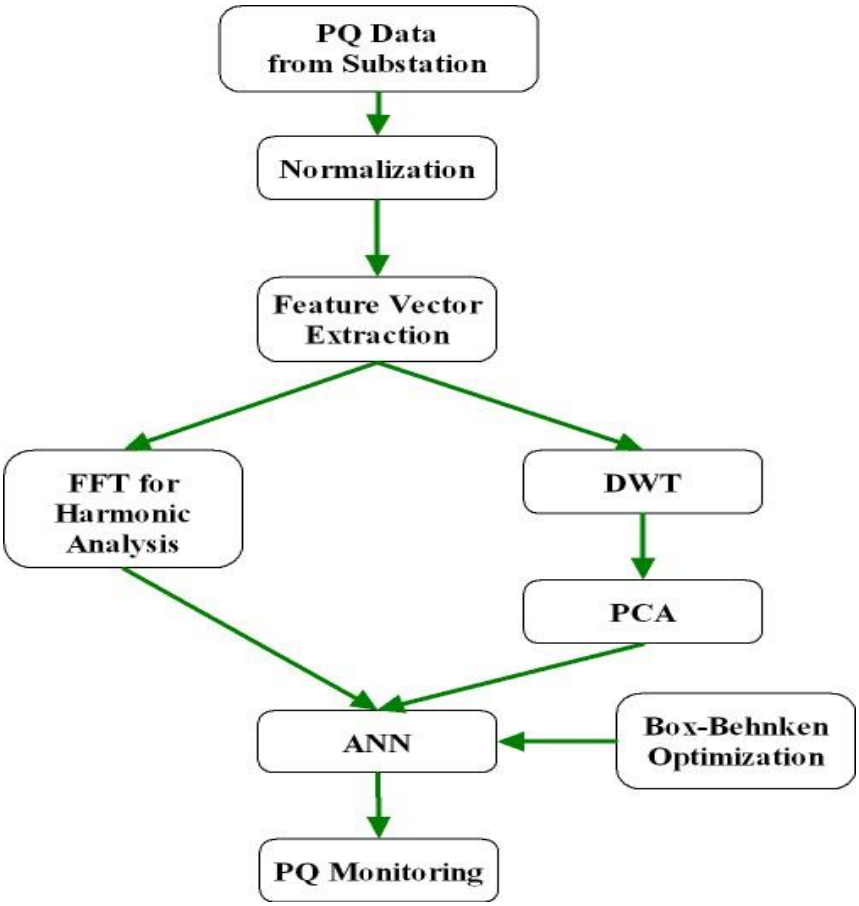

Figure 1 PQ classification and monitoring flow chart

The proposed methodology was tested on both simulated and real data obtained from local substations. The following PQ disturbances (Table 1) are examined.

Table 1 Mathematical models of PQ disturbances

Type of Disturbance	Mathematical Representation	Parameters
Pure sine	$f(t) = A\sin(\omega t + \theta_i)$	A=1, f=50 Hz
Voltage Sag	$f(t) = (1 - \alpha)\sin(\omega t + \theta_i)$	0.1<α<0.9
Voltage Swell	$f(t) = (1 + \alpha)\sin(\omega t + \theta_i)$	0.1<α<0.9
Harmonics	$f(t) = \sin(\omega t + \theta_i) + \alpha_3 \sin(3\omega t + \theta_i) + \alpha_5 \sin(5\omega t + \theta_i) + \alpha_7 \sin(7\omega t + \theta_i)$	0.1<α3<0.9 0.1<α5<0.9 0.1<α7<0.9
Interruption	$f(t) = k_s\sin(\omega t + \theta_i)$	$0<k_s<0.1$
Flicker	$f(t) = \sin(\omega t + \theta_i) + B_v \sin(2\pi f_l t)$	$0.1 \leq B_v \leq 0.2$ $0.1 \leq f_l \leq 0.2$
DC Component	$f(t) = DCe^{(-5t)} + \sin(\omega t + \theta_i)$	$0.1 \leq DC \leq 0.9$
Transient	$f(t) = \sin(\omega t + \theta_i) + 2e^{(-10t)}\sin(2\pi f_t t)$	$2000 \leq f_t \leq 8000$
Electromagnetic Interference	$f(t) = \sin(\omega t + \theta_i) + (emi)\sin(2\pi (emf)t)$	$0.1 \leq emi \leq 0.9$ $1E1 \leq emf \leq 1E9$

*Here ω is radial frequency and equals to 2π*f.*
***fl, ft,* and *emf* represent interrupted, transient and electromagnetic interference signal frequencies, *A, Bv, ks DC*

and *emi* represent magnitude of pure signal, flicker signal, interruption, DC component and electromagnetic interference signal, respectively.

2.1 Signal Processing Methods

PQ disturbances may be divided into two classes: 'steady state disturbances' (long-term and periodic persistence); and 'transient state disturbances' (occurring within milliseconds) and are not inherently static and require time-frequency analysis. In order to investigate the PQ disturbances, the voltage waveform is transformed into different forms by various techniques.

2.2 Fast Fourier Transform

The FFT (Equation 1) has been used to detect harmonics in the PQ data. A rectangular data window over a period covering an integer number of cycles of the fundamental frequency is used.

$$f(n) = \frac{1}{N}\sum_{k=0}^{N-1} f(k)e^{j2\pi nk/N}\ n = 0,1,2,\dots,N-1 \quad (1)$$

where N is total number of samples and $f(k)$ is the PQ signal to be analyzed.

2.3 Discrete Wavelet Transform

The wavelet transform provides time frequency resolution across all frequency ranges with varying window size (wide for low frequencies, narrow for high frequencies). In this study, the wavelet transform is used to determine the distinguishing features from the voltage samples in the data window. The PQ signal is passed through a series of filters in the DWT procedure. First, the input signal (normalized voltage signal) is passed through a low-pass filter using its convolution response with the impulse response of the low-pass filter. The signal is simultaneously separated using a high-pass filter with impulse response h. The most favorable condition was created by reducing it with 2 coefficients as in Equations 2-4.

$$y[n] = (x * g)[n] = \sum_{k=1}^{n} x[k]g[n-k] \quad (2)$$

$$y_{high}[n] = \sum_{k=1}^{n} x[k]h[2n+1-k] \quad (3)$$

$$y_{low}[n] = \sum_{k=1}^{n} x[k]g[2n-k] \quad (4)$$

where $x[k]$ is the sampled PQ data, $h[2n+1-k]$ and $g[2n-k]$ are the high-pass and low-pass filter coefficients and n is the number of samples.

The minimum description length (MDL) criterion was used to select the wavelet function. Shannon entropy was used to find the most suitable resolution level. Accordingly, the entropy of each subspace, approximation (***a***) and detail (***d***) coefficients are calculated at each resolution level of the wavelet. Shannon entropy states that if the entropy of a sine wave at a new level is higher than the previous level, it is not necessary to decompose the sine wave. In this study, the decomposition level was taken as 9 and Daubechies_8 (Db8) was used as the wavelet family.

The energy levels of the detail coefficients were used, as the wavelet transform has time and frequency restrictions. These levels are given by Equation 5.

$$d_{1-9Energy} = \sum_{k=1}^{N/2} d_{1-9}^2 \quad (5)$$

where ***d*** is the detail coefficient for each level. If the equation is rearranged by the normalization process, it can be written as follows.

$$d_{1-9\,norm} = \frac{f_s}{10^6} d_{1-9\,Energy} \quad (6)$$

where f_s is sampling frequency.

Some PQ data is in sine form but the frequency differs from 50Hz. In this situation the energy level of the detail coefficients vary with respect to time. These changes are almost the same as the situation of voltage sag/swell. Therefore, the energy levels of the detail coefficients are then processed with PCA to distinguish between frequency changes and voltage sag/swell.

2.4 Principle Component Analysis

PCA is a linear function that can reduce dimensionality of information in complex data sets, and so is frequently used for analysis in many applications including image processing, pattern recognition, and data reduction. PCA performs a transformation on a complex data set to

produce a data set of reduced size that reveals simplified structure and enables its interpretation. The aim is to determine a coordinate system that reduces the size of the data set to provide meaningful represention with fewer variables and allow multivariate problems to be solved. In other words, for a problem with ***p*** variables, the aim is to reduce the size from p-dimensional space to a k-dimensional space (***k***<***p***) by expressing it with fewer ***k*** variables. If the variables are fully interdependent or independent of each other, there is no benefit in reducing the size because there is equal variance in all dimensions. Principal component analysis may be used to determine the meaningful data. This can be used to re-express a noisy data set to separate signal from noise (He et al., 2011).

If the original data set representing each row is represented by ***X*** (m × n), the resulting matrix is denoted by ***Y*** (m × n) by using linear transformation ***P***. The re-expressed form of ***Y*** is given in Equation 7.

$$\boldsymbol{PX} = \boldsymbol{Y} \tag{7}$$

Let the columns of ***P*** be represented by $\boldsymbol{p_i}$, the rows of ***X*** with $\boldsymbol{x_i}$ and the rows of ***Y*** with $\boldsymbol{y_i}$. According to this presentation, Equations 8-10 are derived.

- ***P*** is a matrix that converts ***X*** into ***Y***.
- Geometrically, ***P*** turns ***X*** into ***Y*** by applying rotation and stretching.
- **P** rows $\{p_1, \ldots, p_m\}$, ***X*** columns $\{x_1, \ldots, x_n\}$ is a set of new vectors to express.

$$PX = \begin{bmatrix} p_1 \\ \vdots \\ p_m \end{bmatrix} [x_1 \quad \cdots \quad x_n] \tag{8}$$

$$Y = \begin{bmatrix} p_1 x_1 & \cdots & p_1 x_n \\ \vdots & \ddots & \vdots \\ p_m x_1 & \cdots & p_m x_n \end{bmatrix} \tag{9}$$

$$y_i = \begin{bmatrix} p_1 x_i \\ \vdots \\ p_m x_i \end{bmatrix} \tag{10}$$

The row vectors $\{p_1, \ldots, p_m\}$, will be the main components of ***X***. The best option should be chosen to re-express ***X*** and linear transformation ***P***.

2.4.1. Singular Value Decomposition (SVD)

In this study, SVD is used to perform the PCA analysis in order to obtain the load and skor matrices of a given set of PQ data. Let $\boldsymbol{X}$ be a random matrix of size n×m and X^TX be a symmetrical square matrix of size $n \times n$.

- $\{\widehat{\boldsymbol{v}}_{\boldsymbol{1}}, \widehat{\boldsymbol{v}}_{\boldsymbol{2}}, \dots, \widehat{\boldsymbol{v}}_{\boldsymbol{r}}\}$, for the XX^T symmetric matrix $\{\lambda_1, \lambda_2, \dots, \lambda_r\}$ is the set of orthonormal m×1 dimensional eigenvectors with their eigenvalues.

$$(X^TX)\hat{v}_i = \lambda_i \hat{v}_i \tag{11}$$

- The value of $\sigma_i \equiv \sqrt{\lambda_i}$ is a positive real number and is called a singular value.
- $\{\widehat{\boldsymbol{u}}_{\boldsymbol{1}}, \widehat{\boldsymbol{u}}_{\boldsymbol{2}}, \dots, \widehat{\boldsymbol{u}}_{\boldsymbol{r}}\}$, is a set of n×1 dimensional vertical vectors defined as $\hat{u}_i \equiv \frac{1}{\sigma_i} X\hat{v}_i$.
- $\hat{u}_i . \hat{u}_j = \delta_{ij}$
- $\|X\hat{v}_i\| = \sigma_i$

The combination of all these features is the application of singular value decomposition. The advantage of singular value decomposition is obtained from the reorganized version of the third item.

$$\sigma_i \hat{u}_i = X\hat{v}_i \tag{12}$$

The product of X with an eigenvector of XX^T is equal to the product of a vector with a scalar value. The eigenvector set $\{\widehat{\boldsymbol{v}}_{\boldsymbol{1}}, \widehat{\boldsymbol{v}}_{\boldsymbol{2}}, \dots, \widehat{\boldsymbol{v}}_{\boldsymbol{r}}\}$ and the vector set $\{\widehat{\boldsymbol{u}}_{\boldsymbol{1}}, \widehat{\boldsymbol{u}}_{\boldsymbol{2}}, \dots, \widehat{\boldsymbol{u}}_{\boldsymbol{r}}\}$ are both orthogonal sets and are based on r-dimensional space. This result can be shown as a matrix product for all vectors.

$$\sum \equiv \begin{bmatrix} \sigma_1 & & & 0 \\ & \ddots & & \\ & & \sigma_r & \\ & & & \ddots \\ 0 & & & 0 \end{bmatrix} \tag{13}$$

$\sigma_1 \geq \sigma_2 \geq \dots \geq \sigma_r$, are sequential sets of singular values. Similarly, V and U orthogonal matrices are created.

$$V = [\hat{v}_{\tilde{1}}\ \hat{v}_{\tilde{2}} \dots\ \hat{v}_{\tilde{m}}] \tag{14}$$

$$U = [\hat{u}_{\tilde{1}}\ \hat{u}_{\tilde{2}} \dots\ \hat{u}_{\tilde{n}}] \tag{15}$$

The vertical vectors $(m - r)$ and $(n - r)$ are added additionally to fill the V and U matrices. The three new matrices can be defined as V, U and $\sum$. Each pair of $\hat{u}_i$ and $\hat{v}_i$ is located along the i

column of the respective matrix. The corresponding singular value σ_i is along the diagonal of the matrix $\sum$ (place *ii*). Thus, the new equation is as shown in Equation 16.

$$XV = U\sum \tag{16}$$

The steps of SVD for PCA are:

- If $x = [x_1, x_2, \dots, x_r]$, x ϵ $\mathbb{R}$ represents the basic vector of $u = [u_1, u_2, \dots, u_n]$ (Orthonormal basis $u_i.u_i = 1$, $u_i.u_j = 0$, i ≠j), it is defined by the most suitable coordinate $(z_1, z_2, \dots, z_k)$, $z_i = (x - \bar{x}).u_i$ represented in the smallest size area.
- First the *m*×*n* size *x* data matrix is read.
- The average value is subtracted from each array of the *x* data matrix.. $(x_c = x - \bar{x})$
- Covariance matrix is calculated.

$$Cov = \frac{1}{m} = \sum_{i=1}^{m} \left(x_{c(i)} - \bar{x}\right)\left(x_{c(i)} - \bar{x}\right)^T \tag{17}$$

- The covariance matrix has Eigenvalues and Eigenvectors. Eigenvectors are selected with the highest Eigenvalues (basic components). As the covariance matrix can be very large and it may take time to find Eigenvectors, singular value decomposition is used to calculate the Eigenvectors.

Feature vectors calculated with the help of wavelet transform and principal component analysis are used to detect voltage sag/swell, interruptions, harmonics and electromagnetic interference, but are not sufficient for flicker. The local largest and largest values of the signal during the flicker can be used as the feature vector. The envelope of the sine wave is obtained by collecting the local largest and is used for the detection of flicker. A number of algorithms have been developed for this. The power frequency range was defined as ± 0.3 Hz, and a flicker frequency range was defined as between 5 and 25 Hz to generate power signals that are randomly generated. The local largest and smallest are calculated.

$$x = x(1 + N * (k - 1): N * k) \tag{18}$$

$$pos(k) = \max(xx) \tag{19}$$

$$neg(k) = \min(xx) \tag{20}$$

2.5 Experimental Design

The Box-Behnken design (BBD) includes a specific subset of factorial combinations from 3k factorial design. In addition, in a BBD, the experimental points are placed in a hypersphere equidistant from the center point and are cornerless (Figure 2) (Ferreira et al., 2007). BBD does

not include full or fractional factorial designs. As BBD contains fewer design points, it is less costly than central composite design.

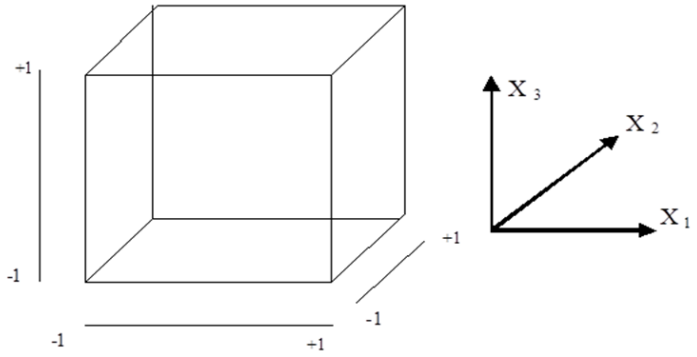

Figure 2 Box-Behnken design limits

BBD is calculated from the basis that an experiment with 3 factors and 3 center points will be performed with 15 experiments. The number of experiments increases as the number of factors increases. As the smallest and largest boundaries of the factors are not contained in this design at the same time, unsuitable non-valued results are prevented from being created by unbalanced values. Box-Behnken design is an answer surface design used in the estimation of 2nd order models, in the design of experiments that are not sequential, and in analyzing the deficiency of the model created. While designing ANN, hidden layer number (HLN), number of neurons used in hidden layer (HLNN), hidden function transfer function (HLTF) and output layer transfer function (OLTF), selection of back propagation algorithm (BPA) are important for the network to make accurate estimation. In this study, Box-Behnken response surface method experiment design was used for the appropriate selection of functions and parameters that form the network. The design needs a total of 46 experiments. The experiment was carried out using the 3-level 5-factor Box-Behnken statistical modeling design. For the level calculation, $2k(k-1)+c_p$ formula was used, 5 for the number of k factors and 7 for the c_p. The levels and factors selected for the artificial neural network created according to the Box-Behnken design are shown in Table 2. A total of 46 experiments were performed in BBD to increase the accuracy of the optimization algorithm. The simplex method is used for optimization for this purpose.

Table 2 Levels selected according to the Box-Behnken design

	Low Level (-1)	**Medium Level (0)**	**High level (+1)**
Hidden Layer Number	1	2	3
Number of Neurons in Hidden Layer	8	10	12
Transfer Function in Hidden Layer	purelin	logsig	tansig
Transfer Function in Output Layer	purelin	logsig	tansig
Back Propagation Algorithm	trainlm	traingd	trainrp

Design factors are coded as -1 (low), 0 (medium) and 1 (high) (Table 2). The response surface method was applied to experimental data obtained using statistical software (Minitab). Linear, quadratic and interaction effects were analyzed to obtain regression polynomial coefficients. The results were analyzed using the specificity coefficient (R^2), variance analysis (ANOVA) and statistical response analysis. ANOVA extends the ***t*** and ***z*** test, which allows the nominal level variable to be in two categories. This test is also called Fisher analysis of variance. Simply, ANOVA gives the determination of optimal ANN structure with the most significant values (i.e. linear, square, and linear by linear interaction terms). The optimal ANN is then formulated as in Equation 21.

$$y = \beta_0 + \beta_1 x_1 + \beta_2 x_2 + \beta_{11} x_1^2 + \beta_{22} x_2^2 + \beta_{12} x_1 x_2 \quad (21)$$

$$\Delta y/\Delta x_1 = \beta_1 + 2\beta_{11} x_1 + \beta_{12} x_2 = 0 \quad (22)$$

$$\Delta y/\Delta x_2 = \beta_2 + 2\beta_{22} x_2 + \beta_{12} x_1 = 0 \quad (23)$$

where x_1 and x_2 are factors, $\beta_0, \beta_1, \beta_2$ are the ANOVA coefficients. The optimum point is found by setting $\Delta y/\Delta x_1$ and $\Delta y/\Delta x_2$ to zero (Eq. 22-23). When the ANOVA table is examined, the regression equation obtained is given in Equation 24. Table 3 shows the regression coefficients for the Box-Behnken design.

Table 3 Regression coefficients for Box-Behnken design

Term	β	SE(β)	t-statistic	p
Constant	0.997943	0.04026	24.790	<0.001
A	0.016844	0.02465	0.683	0.501
B	-0.016836	0.02465	-0.683	0.501
C	0.138255	0.02465	5.608	0.000
D	-0.015959	0.02465	-0.647	0.523
E	-0.003161	0.02465	-0.128	0.899
A*A	0.044750	0.03338	1.341	0.192
B*B	-0.018401	0.03338	-0.551	0.586
C*C	0.137733	0.03338	4.126	0.000
D*D	-0.813495	0.03338	-24.372	0.000
E*E	-0.056295	0.03338	-1.687	0.104
A*B	-0.001955	0.04930	-0.040	0.969
A*C	0.069545	0.04930	1.411	0.171
A*D	0.069180	0.04930	1.403	0.173
A*E	-0.002980	0.04930	-0.060	0.952
B*C	0.053707	0.04930	1.089	0.286
B*D	0.028169	0.04930	0.571	0.573
B*E	-0.013698	0.04930	-0.278	0.783
C*D	-0.042963	0.04930	-0.871	0.392
C*E	0.006440	0.04930	0.131	0.897
D*E	0.013912	0.04930	0.282	0.780

SE: standard error, t-statistics: the value of the t-test result for the respective regression coefficient, p: significance value of the test (S = 0.0986057, PRESS = 0.971302, R-Sq = 96.99%, R-Sq(pred) = 87.98%, R-Sq(adj) = 94.58%)

$$Y = 0.9979 + 0.0003A + 0.0212B + 0.1297C + 0.0328D + 0.0032E + 0.0385A2 - 0.0095B2 + 0.1422C2 - 0.8329D2 - 0.0532E2 - 0.0020A*B + 0.0418A*C + 0.0692A*D - 0.0030A*E - 0.0047B*C + 0.0689B*D - 0.0137B*E - 0.0695C*D + 0.0064C*E + 0.0139D*E \quad (24)$$

The simplex algorithm has been applied to the experimental design (Box-Behnken) to find the most suitable ANN structure. From this process, the MSE of the output was found to be between 0% and 10%. According to this approach, A = -1 (1 hidden layer), B = -1 (number of neurons in hidden layer), C = 0 (logsig), D = 1 (purelin) and E = -1 (trainlm) is the most suitable structure for the ANN, with the smallest MSE value was determined as 0%. This ANN structure was used in the diagnosis of nine PQ disturbances. In the 95% confidence interval Equation 24 can be simplified as follows.

$$Y = 0.9979 + 0.0212B + 0.1297C + 0.0328D + 0.0385A^2 + 0.1422C^2 - 0.8329D^2 - 0.0532E2 + 0.0418A*C + 0.0692A*D + 0.0689B*D - 0.0695C*D \quad (25)$$

Y represents the optimized ANN structure. The Gauss probability density function was applied to the residuals to prove the accuracy of the regression equation and test its conformity to a normal distribution. Figure 3 shows the Gauss probability density function of the residue. Two important parameters (skewness and kurtosis coefficients) were also calculated from this distribution. The skewness value is a measure of the asymmetry of the distribution around the average of the series, which may be (+) or (-). If this value is positive, it indicates asymmetry in the structure of the elements. The skewness coefficient was calculated as 0.18 and this value appears to be between ± 1.96 values in the 95% confidence interval and is in the form of a Gauss distribution. The kurtosis value evaluates the distribution to determine if there is excessive departure from the mean. The kurtosis coefficient was calculated as 2.35, and the proximity to 3 indicates that the curve is Gauss shaped.

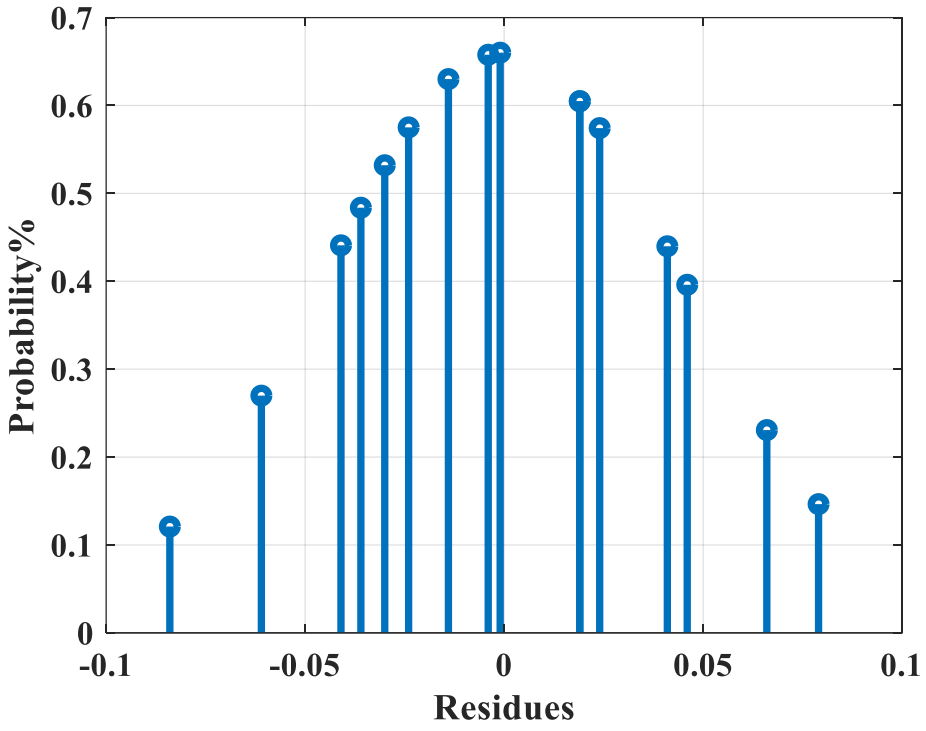

Figure 3 Test of Gauss distribution of the residues

Figure 3 shows the regression model of optimized ANN for PQ disturbances.

2.6 Classification of PQ Disturbances with Optimized ANN

In this study, nine disturbances have been identified from the output layer of an ANN. For this purpose, PQ disturbance data were obtained from substations and the disturbance matrix was estimated. The trained ANN has been tested with nine types of disturbance data (Figure 4). Pure sine, voltage sag/swell, flicker, harmonic, transient, DC component, electromagnetic interference, instantaneous interruption failures were successfully detected by the optimized ANN.

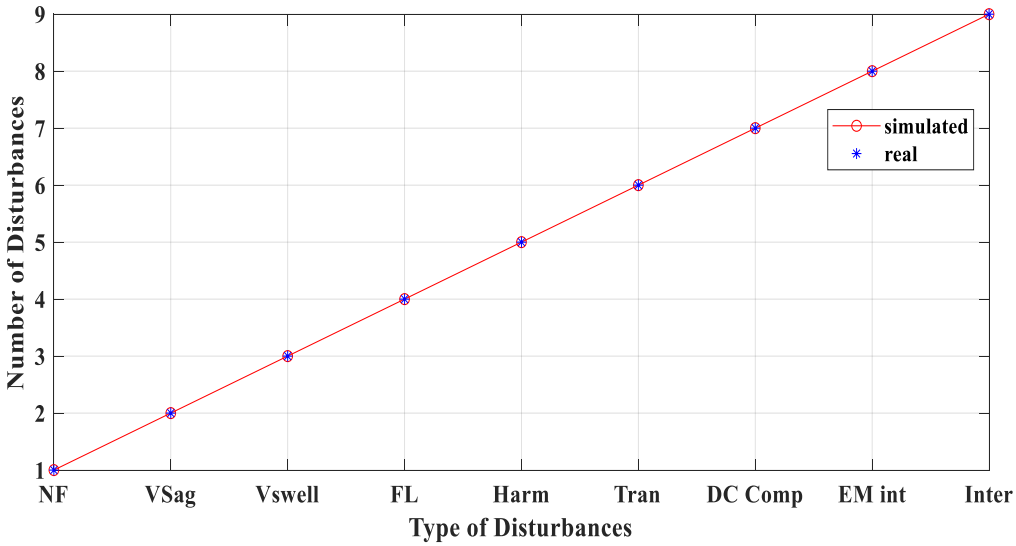

Figure 4 Classification chart of nine disturbances using optimized ANN (100% accuracy)

In Figure 4, NF is no fault, Vsag is voltage sag, Vswell is voltage swell, FL is flicker, Harm is harmonics, Trans is transient condition, DC Comp is DC component, EM Int is electromagnetic interference, and Inter is interruptions. The proposed technique has been shown that it can be used to monitor distribution systems and identify PQ disturbances.

3. CONCLUSION

The proposed study presents a methodology for PQ monitoring consisting of two aspects; feature extraction techniques, and the classification method. Feature extraction techniques included FFT, DWT, PCA, SVD, and experimental design; and classification included optimized ANN methods. The ANN is optimized using simulated data that cover all types of PQ disturbance; the method was then able to distinguish all PQ disturbances in real time data. Nine types of PQ disturbance have been identified, and the techniques have been tested using both simulated and real time data. Results show the technique is able to identify all types of PQ disturbance with an accuracy of 100%.

This study presents the results for one phase of a three phase system. In a real environment the method will be applied to all the phases to obtain the PQ index of each phase. By having multiple monitoring points in a distributed system, the method not only identifies PQ disturbances, but also provides the location and time of the disturbance. This information is helpful for engineers to locate PQ compensating devices in the network.

REFERENCES

Saxena, D. & Verma, K. 2012. Wavelet transform based power quality events classification using artificial neural network and SVM. International Journal of Engineering, Science and Technology.4 (1): 87–96.

Kai, D., Wei, L., Yuchuan, H., Yuchuan, H., Pan, H. & Yimin, Q. 2019. Power Quality Comprehensive Evaluation for Low-Voltage DC Power Distribution System. Proceedings of the IEEE 3rd Information Technology, Networking, Electronic and Automation Control Conference (ITNEC). Chengdu, China.

Shalukho, A.V., Lipuzhin, I.A. & Voroshilov, A.A. 2019. Power Quality in Microgrids with Distributed Generation. Proceedings of the International Ural Conference on Electrical Power Engineering (UralCon), Chelyabinsk, Russia.

Bueno-Contreras, H. & Ramos, G.A. 2019. Optimal Control of an UPQC to assure Power Quality in Electric Distribution Grids. Proceedings of the IEEE Workshop on Power Electronics and Power Quality Applications (PEPQA). Manizales, Colombia.

Rodriguez, A., Ruiz, J.E., Aguado, J., Lopez, J.J., Martin, F.I., & Muñoz, F. 2010. Classification of power quality disturbances using Wavelet and Artificial Neural Networks. Proceedings of the IEEE International Symposium on Industrial Electronics. Bari, Italy.

Chandrasekar, P. & Vijayarajan, K. 2010. Detection and classification of power quality disturbance waveform using MRA based modified wavelet transform and neural networks. Journal of Electrical Engineering. 61 (4): 235–240.

Chen, W., Guo, M., Jin, Q. & Yao, Z. 2019. Reliability Analysis Method of Power Quality Monitoring Device based on Non-Parametric Estimation. Proceedings of the 14th IEEE Conference on Industrial Electronics and Applications (ICIEA). Xi'an, China.

Li, H., Lv, C. & Zhang, Y. 2019. Research on New Characteristics of Power Quality in Distribution Network. Proceedings of the IEEE International Conference on Power, Intelligent Computing and Systems (ICPICS). Shenyang, China.

Ijaz, M., Shafiullah, M. & Abido, M.A. 2015. Classification of power quality disturbances using Wavelet Transform and Optimized ANN. Proceedings of the 18th International Conference on Intelligent System Application to Power Systems (ISAP). Porto, Portugal.

Shilpa, R., Prabhu, S.S. & Puttaswamy, P.S. 2015. Analysis of three phase power quality disturbances. Proceedings of the *International Conference on Emerging Research in Electronics, Computer Science and Technology (ICERECT).* Mandya, India.

Liu, X. & Liu, B. 2015. Recognition of power quality disturbances based on T-S fuzzy logic. Proceedings of the Fifth International Conference on Instrumentation and Measurement, Computer, Communication and Control (IMCCC). Qinhuangdao, China.

Dalai, S., Dey, D., Chatterjee, B., Chakravorti, S. & Bhattacharya, K. 2015. Cross-Spectrum Analysis-Based Scheme for Multiple Power Quality Disturbance Sensing Device. IEEE Sensors Journal. 15 (7): 3989–3997.

Karasu, S. & Başkan, S. 2016. Classification of power quality disturbances by using ensemble technique. Proceedings of the 24th Signal Processing and Communication Application Conference (SIU2016). Zonguldak, Turkey.

Perez, R.S., Oviedo, A.C., Camarillo-peñaranda, J. & Ramos, G. 2016. A Novel Fault Classification Method Using Wavelet Transform and Artificial Neural Networks. Proceedings of the 17th International Conference on Harmonics and Quality of Power (ICHQP). Belo Horizonte, Brazil.

Mejia-Barron, A., Amezquita-Sanchez, J.P., Dominguez-Gonzalez, A., Valtierra-Rodriguez, M., Razo-Hernandez, J.R. & Granados-Lieberman, D. 2017. A scheme based on PMU data for power quality disturbances monitoring. Proceedings of the 43rd Annual Conference of the IEEE Industrial Electronics Society. Beijing, China.

Mohan, N., Soman, K.P. & Vinayakumar, R. 2017. Deep Power : Deep Learning Architectures for Power Quality Disturbances Classification. Proceedings of the International Conference on Technological Advancements in Power and Energy (TAP

Energy). Kollam, India.

Das, D., Chakravorti, T. & Dash, P.K. 2017. Hilbert huang transform with fuzzy rules for feature selection and classification of power quality disturbances. Proceedings of the 4th IEEE Uttar Pradesh Section International Conference on Electrical, Computer and Electronics (UPCON). Mathura, India.

Singh, U. & Singh, S.N. 2017. Application of fractional Fourier transform for classification of power quality disturbances. IET Science, Measurement Technology. 11 (1): 67–76.

Camarillo-Peñaaranda, J.R. & Ramos, G. 2018. Characterization of sags due to faults in radial systems using three-phase voltage ellipse parameters. *IEEE Transactions on Industry Applications*. 54 (3): 2032-2040.

He, R., Hu, B., Zheng, W. & Kong, X. 2011. Robust Principal Component Analysis Based on Maximum Correntropy Criterion. IEEE Transactions on Image Processing. 20 (6): 1485-1494.

Ferreira, S.L.C., Bruns, R.E., Ferreira, H.S., Matos, G.D., David, J.M., Brandão, G.C., da Silva, E.G.P., Portugal, L.A., dos Reis, P.S., Souza, A.S. & dos Santos, W.N.L. 2007. Box-Behnken design: An alternative for the optimization of analytical methods. Analytica Chimica Acta. 597 (2): 179-186.